

Real-time American Sign Language Recognition Using Wrist-worn Motion and Surface EMG Sensors

Jian Wu*, Zhongjun Tian*, Lu Sun*, Leonardo Estevez[§] and Roozbeh Jafari*

*Department of Electrical Engineering, University of Texas at Dallas, Richardson, TX, USA

[§]Texas Instruments Incorporated, Dallas, TX, USA

*{jian.wu, zhongjun.tian, lu.sun2, rjafari}@utdallas.edu

[§]leonardo@ti.com

Abstract—A Sign Language Recognition (SLR) system enables communication between hearing disabled individuals and those who can hear and speak. With the prevalence of the wearable computers, this technology is becoming an important human computer interface capable of reading hand gestures and inferring user's intent. In this paper, we propose a real-time American SLR system leveraging fusion of surface electromyography (sEMG) and a wrist-worn inertial sensor at the feature level. A feature selection is provided for 40 most commonly used words and for four subjects. The experimental results show that after feature selection and conditioning, our system achieves 95.94% recognition rate. The results also illustrate the fusion of two modalities perform better than using only the inertial sensor. We observed that only one channel of sEMG (out of four) located on the wrist and under the wrist-watch is sufficient.

Keywords—Sign language recognition; inertial sensor; sEMG; feature selection

I. INTRODUCTION

Sign language enables deaf and mute persons to communicate with each other using their body language [1]. A sign language recognition (SLR) system serves as an important assistive tool to bridge the communication gap between this community and individuals who do not know sign language by translating the sign language into text or speech [2, 3]. SLR can also be used as a reference design for a gesture based human computer interface (HCI), which shares the same principles and is widely used in human daily life [4-6]. SLR is widely studied in the area of the computer vision and glove-based gesture recognition with the camera and sensing glove as the gesture capture modalities, respectively [7-10]. Vision based SLR can suffer from bad performance in poor lighting conditions and the videos/images captured may be considered invasive to the user's privacy. The glove-based SLR requires an expensive sensing glove, which makes it less ideal for a broad set of applications.

The low cost inertial measure unit (IMU), which consists of a 3-axis accelerometer and 3-axis gyroscope, has been widely studied for gesture recognition by measuring the accelerations and angular velocities of the hand and arm [11, 12]. At the same time, a surface electromyographic sensor (sEMG) measures electrical potentials generated by muscle activities and can be used to distinguish various hand and finger movements based on different muscle activities [13, 14]. The inertial sensor based system is capable of capturing hand orientations and hand and arm movements during the gesture while the sEMG is good at measuring of finger movements and the muscle activity patterns

for the hand and arm. They can be complementary to each other and the fusion of these two systems will enhance the recognition accuracy for different signs, thus making the recognition of large vocabulary of signs easier [15].

In this paper, we propose a real-time American SLR system by fusing inertial sensor modalities and the sEMG modality at the feature level. Our work has the following contributions: 1) Propose an online auto segmentation technique using sEMG; 2) An information gain based filter feature selection method is applied to select the best subset of the features that will enhance the recognition performance; 3) Four different classification algorithms are tested with inter and intra-subject training-testing.

The remainder of this paper is organized as follows. The related work is reviewed in Section II. Our proposed sEMG and inertial sensing hardware devices are introduced in Section III. The signal processing and fusion techniques are explained in Section IV, followed by the experimental results in Section V. Finally, the conclusion is provided in Section VI.

II. RELATED WORK

Sign language recognition using accelerometers and sEMG is studied in several investigations. The performance of the accelerometer based and the sEMG based system is compared in the detection of functional motion activities [16]. Each modality has its own advantages to detect specific activities and the potential of increasing the detection accuracy by fusing these two modalities is explored. It is demonstrated that 5% - 10% accuracy improvement is achieved in the recognition of certain wrist and finger gestures leveraging the fusion of the accelerometer and sEMG data [17]. An effective feature set based on sample entropy is proposed and the recognition accuracy of 93% is reported for 60 Greek sign words using only one feature set for both sEMG and accelerometer data [18]. A framework for Chinese sign language recognition based on accelerometer and EMG sensors is investigated [19]. Auto segmentation is performed to divide continuous sentences into individual words based on the intensity of the sEMG signals. Multi-stage decision level fusion is performed to recognize 120 Chinese words with two hands. At the first stage, the sEMG is used to capture the hand shape and the accelerometer data is used to distinguish the hand orientation. The LDA classifier is used for these two tasks. The cascade sEMG and accelerometer features are incorporated leveraging a multi-stream hidden Markov model (MSHMM) to evaluate complete movements. In the second stage, the first stage decisions are fused with a Gaussian mixture model (GMM) model. Although this

framework achieves a 96.5% accuracy, multi-stage and multiple classifiers will be very computational expensive and would not be suitable for wearable computers with their low-power processors. A feature level fusion approach is introduced to recognize 7 German sign language words [20]. This fusion technique achieves 99.82% accuracy with 1-channel sEMG and one 3-D accelerometer. However, this work does include auto-segmentation. Hence, it cannot be operated in real-time and on-line. Our work differs from the previous work in the following aspects: 1) Propose an adaptive on-line and real-time segmentation technique using sEMG. This is particularly important as users, due to their diverse muscle strengths, exhibit different signal strengths on their sEMG. 2) An information gain filter based feature selection technique is applied and the gyroscope information is incorporated. 3) Our real-time system is evaluated with 40 most commonly used American Sign Language words and best sEMG channels (in our investigation the one located on the wrist) are highlighted.

III. HARDWARE DESCRIPTION

A. Motion Sensor

Fig. 1 shows our 9-axis motion sensor with a size of 1"x1.5". An InvenSense MPU9150 9-axis MEMS sensor is used to measure the 3-axis acceleration, 3-axis angular velocity and 3-axis magnetic strength. A Texas Instruments (TI) 16-bit low power microcontroller, MSP430F5528, is used as the central processor. A dual mode Bluetooth unit from Blueradios and a microSD module are available on-board. The user can choose to stream the data to a PC/tablet for real-time processing or log the data onto a microSD card. A charging circuit is included.

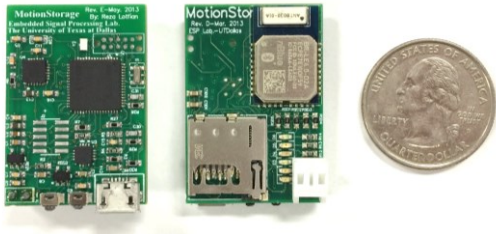


Fig. 1. Motion Sensor Board.

In this paper, the sampling frequency is set to 100 Hz and measurement range of accelerometer and gyro are $\pm 2g$ and $\pm 250 \frac{\text{degrees}}{\text{second}}$. This is enough to capture movements associated with the sign language.

B. sEMG hardware platform

sEMG is a non-invasive technique to measure the electrical potential of muscle activities. Our lab developed 16 channel physiological signal acquisition system, shown in Fig. 2, for ECG, EEG and sEMG. The system is used as a 4-channel sEMG in this investigation [21]. TI ADS1299 analog front end is used to capture 4-channel sEMG and a TI MSP430 microcontroller collects data and forwards it to the Bluetooth module. The data is transmitted to a PC via Bluetooth. A gain of 1 is used on the ADS1299 to support a resolution of roughly $0.4 \mu V$. Patch-based electrodes are attached to the forearm to capture the sEMG signals.

Generally, the sEMG signal peak-to-peak voltage ranges from 0 to 10mV [22]. Prior investigations have reported that the frequency components of sEMG is typically 0-500 Hz depending on the electrode spacing, the amount of fatty tissue and muscle type [23]. Therefore, we set the sampling frequency for sEMG at 1 kHz to satisfy the Nyquist sampling criterion.



Fig. 2. 8-channel sEMG board.

IV. SIGNAL PROCESSING AND FUSION

Fig. 3 shows the block diagram of the proposed real-time system for the ASL recognition fusing inertial measurements and sEMG signals. In the training phase, the preprocessing incorporates filtering and noise rejection. The preprocessing could also include other services like time synchronization if needed. The automatic segmentation is applied to both streams to extract the period during which the sign gesture is performed. After the segmentation, a set of features are extracted for each individual modality (inertial and sEMG) separately. The two feature sets are cascaded into one feature vector before the feature selection is performed with a filter based feature selection technique for four classification algorithms (*i.e.* decision tree, support vector machine, NaïveBayes and nearest neighbor). The best feature subset is selected and the best classification model is determined based on the selected feature subset. In the testing phase, the same preprocessing and segmentation approaches as in the training phase are used. The selected features are extracted from two modalities and the prediction result is obtained with the trained prediction and classification model.

A. Preprocessing

It is important to synchronize the motion sensor data and sEMG data before fusing them. In our system, two data streams are sent to a PC using Bluetooth and all the samples are time stamped with the local PC clock. Although the delay between sensors and PC varies, this small error is considered to be negligible (a 5-20ms typical delay for Bluetooth) and the synchronization approach used is sufficient for our application. The sEMG signal is affected by several low frequency noise sources. The power density function of sEMG beyond the range of 5Hz – 450Hz is negligible and a 5Hz high pass filter is applied as suggested in a prior work [24]. We chose a sixth-order IIR filter. For the accelerometer and gyroscope data, the raw signal readings are used.

B. Segmentation

For the real-time scenario, an automatic segmentation is very important to define the start and the end of the sign gesture so that the correct features can be extracted prior to classification. The sEMG signals are used to perform the online segmentation in our paper.

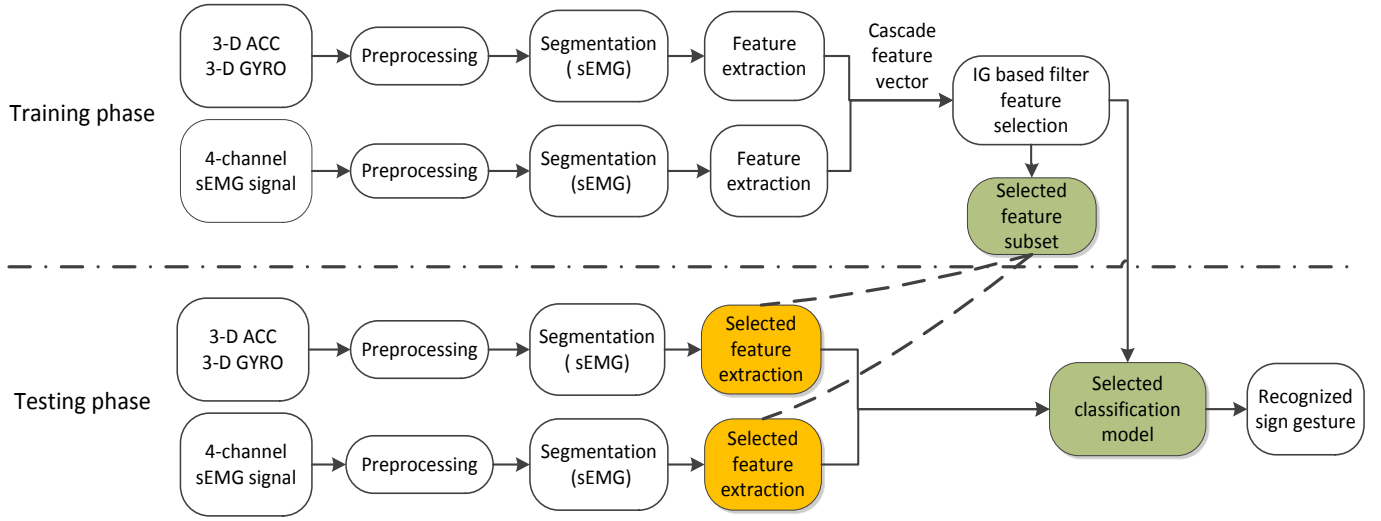


Fig. 3. Diagram of proposed system.

The proposed data segmentation approach is described as follows. The average energy, E , of the 4-channel sEMG signals are calculated in a moving non-overlapping window according to (1). N is the total number of channels, n is the sample number in the window and $s_c(i)$ is the sample number i of sEMG signal from channel c . The window size is chosen as 128 millisecond. Each window contains 128 samples as the sampling frequency for sEMG is set at 1000Hz.

$$E = \frac{1}{n} \sum_{i=1}^n \sum_{c=1}^N s_c^2(i) \quad (1)$$

If the average energy of five continuous windows are all larger than a threshold T , the starting time of the first window is chosen as the beginning of the segmentation. The ending time of the segmentation is determined when the average energy of three continuous windows are all smaller than the threshold T . These methods are refined and the values are determined empirically. It is important to choose a suitable threshold to perform the correct segmentation. However, different users have different muscle strengths, and a pre-defined threshold may not work well for different subjects. We use an adaptive threshold detection technique that will adjust the threshold for different users and different noise levels. Our adaptive threshold detection technique is described as follows: 1) Calculate average energy, E , for 5 continuous windows. 2) If $E < a * T$, the user is considered to have no muscle activity and the threshold is updated with $T = b * E$. The initial value of a , b and T are chosen as 0.5, 4 and 0.008, respectively based on training on 4 subjects. The initial threshold 0.008 is much bigger than the average energy of all subjects when there is no muscle activity and a controls the rate of reducing threshold when a period with a smaller muscle activity is detected while b controls the rate of enlarging threshold in case the noise level increases.

C. Feature Extraction

Various features are investigated in previous works for both sEMG and inertial sensors for gesture and activity recognition tasks. In the training phase, we extract a large number features

for both sEMG and inertial sensors [25-29]. Tables I and II list the features used in our investigation for sEMG and inertial sensors. For the sEMG, all features listed are extracted for each channel and the dimension of the feature vector for 4 channels is 76. For the inertial sensor, the features chosen are extracted for all 3 axes of accelerometer, 3 axes of gyroscope and the magnitude of the accelerometer and gyroscope, resulting a feature vector with the dimension $24 * 8 = 192$. The extracted sEMG features and inertial sensor features are cascaded into a final vector with a dimension of 268.

TABLE I. SEMG FEATURES

Feature name (dimension)	Feature name (dimension)
Mean Absolute Value (1)	Variance (1)
Four order Reflection Coefficients (4)	Willison Amplitude in 5 amplitude ranges (5)
Histogram (1)	Modified Median Frequency (1)
Root Mean Square (1)	Modified Mean Frequency (1)
Four order AR coefficients (4)	

TABLE II. INERTIAL SENSOR FEATURES

Feature name (dimension)	Feature name (dimension)
Mean (1)	Variance (1)
Standard Deviation (1)	Integration (1)
Root Mean Square (1)	Zero Cross Rate (1)
Mean Cross Rate (1)	Skewness (1)
Kurtosis (1)	First three orders of 256-point FFT Coefficients (3)
Entropy (1)	Signal Magnitude Area (1)
AR coefficients (10)	

D. Feature Selection

A feature selection technique is used to remove redundant and irrelevant features and determine the best subset of features. It is challenging to determine which features are better for a certain task and it is necessary to do feature selection. Reducing the number of features will also reduce the computational complexity which will be of interest for real-time signal processing on low-power wearable computers.

There are three different methods of feature selection: filter methods, wrapper methods, and embedded methods [30]. In this paper, we choose an information gain (IG)-based filter method along with a ranking algorithm which ranks all the features based on the IG criterion. Unlike the wrapper method, this method can operate irrespective of the choice on the classification algorithm and its performance is not impacted by the classification algorithm.

E. Classification

In this paper, we investigate four most commonly used classification algorithms: decision tree (J48) [31], support vector machine (LibSVM) [32], nearest neighbor and NaiveBayes. An open source machine learning tool called Weka is used for the implementation of the classification tasks [33]. The RBF kernel is applied for the LibSVM and the grid search algorithm is used to determine the best parameters for the kernel. For all other classification techniques, the default model of Weka is used.

V. EXPERIMENT SETUP AND RESULTS

A. Sensor Placement

Fig. 4 shows the sensor placement for our experiments. Both sEMG and inertial sensors are placed on the right forearm to capture one-hand signs. The inertial sensor is placed on the wrist which is the common location for wrist-worn watches while 4-channel sEMG electrodes are placed on four muscle groups on the forearm: (1) extensor digitorum, (2) flexor carpi radialis longus, (3) extensor carpi radialis longus and (4) extensor carpi ulnaris. Reference and bias electrodes are placed on the right upper arm far from 4 channel electrodes. To capture sEMG signals more effectively, a bi-polar configuration is used for each channel and the distance between two electrodes is chosen at 15 mm [34]. Fig. 4 shows the electrode patch positions for four sEMG channels.

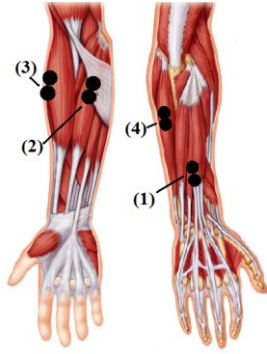


Fig. 4. Placement of sEMG electrodes.

B. Dataset

In this investigation, we consider 40 most commonly used words in daily conversations from the American Sign Language vocabulary. Four healthy subjects participated in the data collection. For each subject, the data is collected in three trials on different days. The subjects were asked to perform each sign 25 times during each trial. Fig. 5 shows the system setup for the data collection.

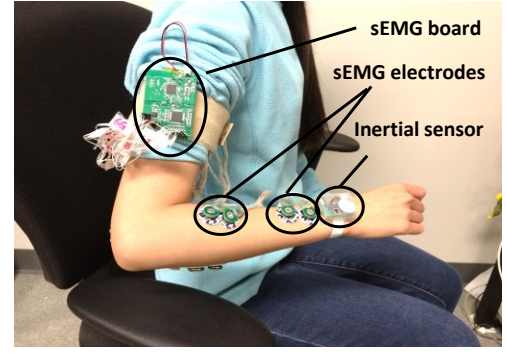


Fig. 5. System setup for data collection.

C. Experiments

To evaluate the performance of our system, three different scenarios are considered: 1) Self cross validation (SCV): 10-fold cross validation is performed for dataset acquired from each subject. This scenario usually offers the best accuracy of one subject. 2) All cross validation (ACV): the data from 4 subjects are combined and the 10-fold cross validation is applied. The feature selection is performed considering data for all subjects which offers a good generalization for the classification technique. 3) Leave one subject out test: the model is trained using data from three subjects and is tested on the data acquired from the fourth user. This scenario evaluates how well the model performs when the classifier is not (re)trained for a new user. Considering diverse muscle profiles in users, we expect to see the least ideal recognition rates in this scenario.

D. Feature selection results

The features are ranked using the information gain criterion. The features with the highest ranking are selected to form a feature subset. To determine the best size of the feature subset, the ACV is performed on four classification techniques as the size of the feature subset increases from 10 to 268.

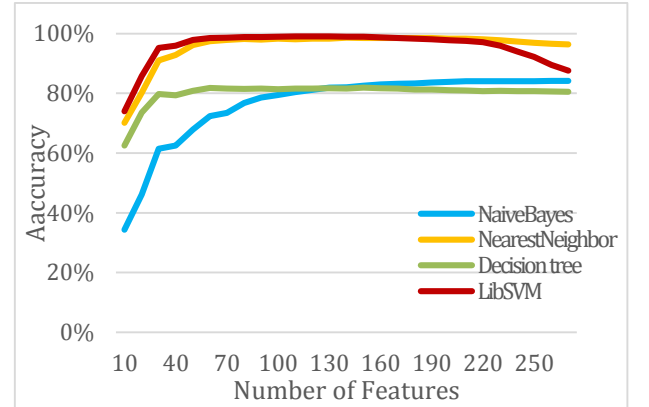


Fig. 6. Results of feature selection.

TABLE III. MAXIMUM DATA POINT OF FEATURE SELECTION

Classifier	Maximum (feature number, accuracy)
NaiveBayes	(260, 84.11%)
NearestNeighbor	(180, 98.56%)
Decision Tree	(150, 81.88%)
LibSVM	(130, 99.09%)

Fig. 6 shows the classification accuracy as the number of features increases and Table III shows the data points illustrating the highest accuracy. From the results, we can see that as the number of features increases, the accuracy of classification increases. However, when the feature size exceeds 130 and 180 for LibSVM and Nearest Neighbor, respectively, the accuracy begins to decrease which is due to over-fitting. When the feature size reaches 30, LibSVM offers an accuracy of 95.94%. Considering the limited computational resources in low-power wearable computers, we settled for the best 30 features. Table IV shows the number of features selected from each sensor. Most features are from the accelerometer which captures the gravity and acceleration caused by motion. Gravity on the accelerometer plays a major role as it can reveal the hand orientation. Nine gyroscope features are selected which indicates the hand and arm rotation are also important. There are only 3 sEMG features selected which indicates for the most commonly used signs we considered, the sEMG is not as significant as the inertial sensor.

TABLE IV. NUMBER OF SELECTED FEATURES FROM SENSORS

	Accelerometer	Gyroscope	sEMG
Number of Features	18	9	3

We also made an interesting observation that all selected sEMG features are from one electrode placed on the wrist where normally a wrist watch sits. This electrode measures extensor digitorum muscle activities near the wrist. This observation leads to the conclusion that only one sEMG electrode would be sufficient for the ultimate deployment.

E. Classification results

Fig. 7 shows the SCV results of all four subjects. The figure shows LibSVM and nearest neighbor classifiers obtain a high accuracy for all four subjects while the decision tree and naïve Bayes classifiers achieve lower accuracy. For all subjects, the accuracies of different classifiers are stable and consistent. These results indicate that if we train the classifier for individual subjects, the system will achieve a high accuracy for the 40 American Sign Language words. This performance may vary slightly from subject to subject which is mainly due to the fact that the subjects are first time learners of the sign language and may not have developed necessary skills to perform the hand gestures very well.

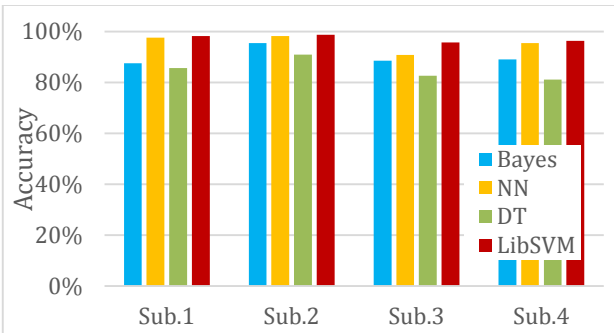


Fig. 7. Result of self-cross validation (SCV).

In Fig. 8, the cross validation results for all subjects are presented. Various classifiers have significantly different performance, and the LibSVM obtains the best accuracy at

95.14%. In this figure, the classification accuracies with sEMG and without sEMG are illustrated. We observe that sEMG enhances the classification accuracy for all scenarios. However, the improvement is not significant which indicates that the inertial sensor plays a major role in discriminating different signs.

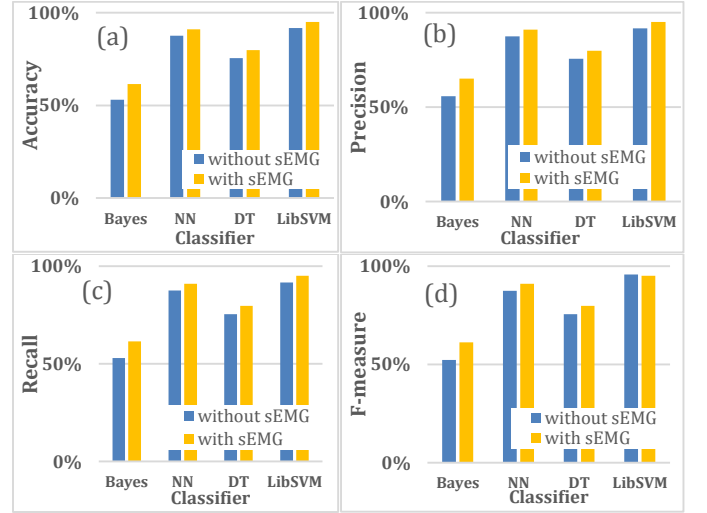


Fig. 8. Results of all cross validation (ACV).

Fig. 9 shows the leave one subject out test results. The *X-axis* is the subject that is left out, and the *Y-axis* shows the accuracy for various classifiers. None of the classifiers can provide high accuracy for detection of the 40 signs. LibSVM still provides the highest accuracy among the four classifiers. There are two possible reasons for the low accuracy. 1) All subjects are new learners and never had prior experience with the sign language. Even though they followed the instructions, the gestures for the same words are different from subject to subject. 2) Various users have very different muscle strength and therefore, the observed signals will be impacted due to their physical conditions. In future, we will further investigate the causes for this observation. The real-time operation of our system may be viewed at: <http://tiny.cc/6uaivx>.

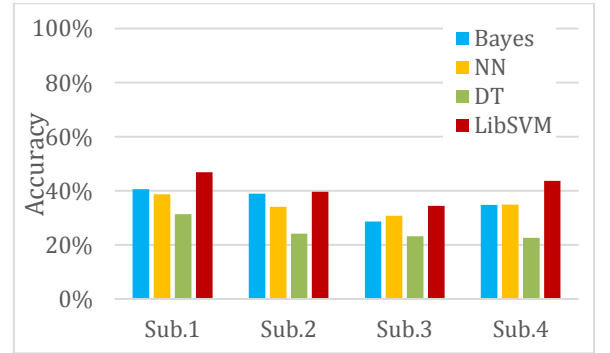


Fig. 9. Result of leave one subject out test.

VI. CONCLUSION

In this paper, we proposed a real time multimodal American Sign Language recognition system using a feature level fusion scheme. A broad set of features from both sEMG and inertial

sensors were considered and an information gain based filter method is applied to the feature selection along with a ranking algorithm. We evaluated our system with 40 mostly common used signs in the daily conversation by comparing the performance of four different classifiers. Our system achieves high accuracy when it is trained for each individual subject. In future, we will extend the recognition for a larger number of signs. We will consider placing our proposed devices on two hands and will evaluate the signal processing performance.

ACKNOWLEDGMENT

This work was supported in part by the National Science Foundation, under grant CNS-1150079, and Texas Instruments Inc. Any opinions, findings, conclusions, or recommendations expressed in this material are those of the authors and do not necessarily reflect the views of the funding organizations.

REFERENCES

- [1] W. C. Stokoe, "Sign language structure: An outline of the visual communication systems of the american deaf," *Journal of deaf studies and deaf education*, vol. 10, no. 1, pp. 3–37, 2005.
- [2] D. Barberis, N. Garazzino, P. Prinetto, G. Tiotto, A. Savino, U. Shoaib, and N. Ahmad, "Language resources for computer assisted translation from italian to italian sign language of deaf people," in *Proceedings of Accessibility Reaching Everywhere AEGIS Workshop and International Conference, Brussels, Belgium (November 2011)*, 2011.
- [3] A. B. Grieve-Smith, "Signsynth: A sign language synthesis application using web3d and perl," in *Gesture and Sign Language in Human-Computer Interaction*, pp. 134–145, Springer, 2002.
- [4] C. Manresa, J. Varona, R. Mas, and F. Perales, "Hand tracking and gesture recognition for human-computer interaction," *Electronic letters on computer vision and image analysis*, vol. 5, no. 3, pp. 96–104, 2005.
- [5] K. Oka, Y. Sato, and H. Koike, "Real-time fingertip tracking and gesture recognition," *Computer Graphics and Applications, IEEE*, vol. 22, no. 6, pp. 64–71, 2002.
- [6] K. Liu, C. Chen, R. Jafari, and N. Kehtarnavaz, "Fusion of inertial and depth sensor data for robust hand gesture recognition," 2014.
- [7] T. Starner, J. Weaver, and A. Pentland, "Real-time american sign language recognition using desk and wearable computer based video," *Pattern Analysis and Machine Intelligence, IEEE Transactions on*, vol. 20, no. 12, pp. 1371–1375, 1998.
- [8] C. Vogler and D. Metaxas, "A framework for recognizing the simultaneous aspects of american sign language," *Computer Vision and Image Understanding*, vol. 81, no. 3, pp. 358–384, 2001.
- [9] T. E. Starner, "Visual recognition of american sign language using hidden markov models," tech. rep., DTIC Document, 1995.
- [10] C. Oz and M. C. Leu, "American sign language word recognition with a sensory glove using artificial neural networks," *Engineering Applications of Artificial Intelligence*, vol. 24, no. 7, pp. 1204–1213, 2011.
- [11] A. Y. Benbasat and J. A. Paradiso, "An inertial measurement framework for gesture recognition and applications," in *Gesture and Sign Language in Human-Computer Interaction*, pp. 9–20, Springer, 2002.
- [12] O. Amft, H. Junker, and G. Troster, "Detection of eating and drinking arm gestures using inertial body-worn sensors," in *Wearable Computers, 2005. Proceedings. Ninth IEEE International Symposium on*, pp. 160–163, IEEE, 2005.
- [13] A. B. Ajiboye and R. F. Weir, "A heuristic fuzzy logic approach to emg pattern recognition for multifunctional prosthesis control," *Neural Systems and Rehabilitation Engineering, IEEE Transactions on*, vol. 13, no. 3, pp. 280–291, 2005.
- [14] J.-U. Chu, I. Moon, and M.-S. Mun, "A real-time emg pattern recognition based on linear-nonlinear feature projection for multifunction myoelectric hand," in *Rehabilitation Robotics, 2005. ICORR 2005. 9th International Conference on*, pp. 295–298, IEEE, 2005.
- [15] Y. Li, X. Chen, X. Zhang, K. Wang, and J. Yang, "Interpreting sign components from accelerometer and semg data for automatic sign language recognition," in *Engineering in Medicine and Biology Society, EMBC, 2011 Annual International Conference of the IEEE*, pp. 3358–3361, IEEE, 2011.
- [16] D. Sherrill, P. Bonato, and C. De Luca, "A neural network approach to monitor motor activities," in *Engineering in Medicine and Biology, 2002. 24th Annual Conference and the Annual Fall Meeting of the Biomedical Engineering Society EMBS/BMES Conference, 2002. Proceedings of the Second Joint*, vol. 1, pp. 52–53, IEEE, 2002.
- [17] X. Chen, X. Zhang, Z.-Y. Zhao, J.-H. Yang, V. Lantz, and K.-Q. Wang, "Hand gesture recognition research based on surface emg sensors and 2d-accelerometers," in *Wearable Computers, 2007 11th IEEE International Symposium on*, pp. 11–14, IEEE, 2007.
- [18] V. E. Kosmidou and L. J. Hadjileontiadis, "Sign language recognition using intrinsic-mode sample entropy on semg and accelerometer data," *Biomedical Engineering, IEEE Transactions on*, vol. 56, no. 12, pp. 2879–2890, 2009.
- [19] Y. Li, X. Chen, X. Zhang, K. Wang, and Z. J. Wang, "A sign-component-based framework for chinese sign language recognition using accelerometer and semg data," *Biomedical Engineering, IEEE Transactions on*, vol. 59, no. 10, pp. 2695–2704, 2012.
- [20] J. Kim, J. Wagner, M. Rehm, and E. André, "Bi-channel sensor fusion for automatic sign language recognition," in *Automatic Face & Gesture Recognition, 2008. FG'08. 8th IEEE International Conference on*, pp. 1–6, IEEE, 2008.
- [21] V. Nathan, J. Wu, C. Zong, Y. Zou, O. Dehzangi, M. Reagor, and R. Jafari, "Demonstration paper: A 16-channel bluetooth enabled wearable eeg platform with dry-contact electrodes for brain computer interface," in *ACM International Conference on Wireless Health*, 2013.
- [22] L. K. Yun, T. T. Swee, R. Anuar, Z. Yahya, A. Yahya, and M. R. A. Kadir, "Sign language recognition system using semg and hidden markov model," 2013.
- [23] C. J. De Luca, L. Donald Gilmore, M. Kuznetsov, and S. H. Roy, "Filtering the surface emg signal: Movement artifact and baseline noise contamination," *Journal of biomechanics*, vol. 43, no. 8, pp. 1573–1579, 2010.
- [24] R. Merletti and P. Di Torino, "Standards for reporting emg data," *J Electromyogr Kinesiol*, vol. 9, no. 1, pp. 3–4, 1999.
- [25] A. Phinyomark, C. Limsakul, and P. Phukpattaranont, "A novel feature extraction for robust emg pattern recognition," *arXiv preprint arXiv:0912.3973*, 2009.
- [26] M. Zhang and A. A. Sawchuk, "Human daily activity recognition with sparse representation using wearable sensors," *Biomedical and Health Informatics, IEEE Journal of*, vol. 17, no. 3, pp. 553–560, 2013.
- [27] S. H. Khan and M. Sohail, "Activity monitoring of workers using single wearable inertial sensor,"
- [28] O. Paiss and G. F. Inbar, "Autoregressive modeling of surface emg and its spectrum with application to fatigue," *Biomedical Engineering, IEEE Transactions on*, no. 10, pp. 761–770, 1987.
- [29] A. M. Khan, Y.-K. Lee, S. Y. Lee, and T.-S. Kim, "A triaxial accelerometer-based physical-activity recognition via augmented-signal features and a hierarchical recognizer," *Information Technology in Biomedicine, IEEE Transactions on*, vol. 14, no. 5, pp. 1166–1172, 2010.
- [30] I. Guyon and A. Elisseeff, "An introduction to variable and feature selection," *The Journal of Machine Learning Research*, vol. 3, pp. 1157–1182, 2003.
- [31] J. R. Quinlan, *C4.5: programs for machine learning*. Elsevier, 2014.
- [32] C.-C. Chang and C.-J. Lin, "LIBSVM: A library for support vector machines," *ACM Transactions on Intelligent Systems and Technology*, vol. 2, pp. 27:1–27:27, 2011. Software available at <http://www.csie.ntu.edu.tw/~cjlin/libsvm>.
- [33] M. Hall, E. Frank, G. Holmes, B. Pfahringer, P. Reutemann, and I. H. Witten, "The weka data mining software: an update," *ACM SIGKDD explorations newsletter*, vol. 11, no. 1, pp. 10–18, 2009.
- [34] M. Z. Jamal, "Signal acquisition using surface emg and circuit design considerations for robotic prosthesis," 2012.